Circular RNA 0004904 promotes autophagy and regulates the fused in sarcoma/vascular endothelial growth factor axis in preeclampsia

WEI DAI and XINGHUI LIU

Department of Obstetrics, West China Hospital of Sichuan University, Chengdu, Sichuan 610041, P.R. China

Received November 22, 2020; Accepted March 16, 2021

DOI: 10.3892/ijmm.2021.4944

Abstract. Circular (circ)RNA has been demonstrated to serve crucial roles in cell proliferation, differentiation and autophagy. However, to date, the function and mechanism of action of circRNA in preeclampsia have not been reported. The present study aimed to analyze the roles of circRNA-0004904 in preeclampsia and to clarify its underlying pathogenic mechanism. The expression levels of circ-0004904, microRNA (miR)-570 and autophagy-related 12 (ATG12) were detected by reverse transcription-quantitative (RT-q)PCR. In addition, the protein levels of ATG12, vascular endothelial growth factor (VEGF) and fused in sarcoma (FUS) were determined by western blot assay. The distribution of mRFP-GFP-LC3 in HTR8 and JEG3 cells was analyzed by confocal microscopy. Fluorescence *in situ* hybridization assay was utilized to identify the colocalization of circ-0004904 and miR-570. Cell proliferation was determined by 5-ethynyl-2'-deoxyuridine assay, and invasion was evaluated by Matrigel invasion assay. The results of the present study demonstrated that the expression levels of circ-0004904 were elevated in the placental tissues and plasma samples of patients with preeclampsia compared with those in the control group samples. Ectopic expression of circ-0004904 promoted autophagy, but inhibited migration and proliferation of HTR8 cells compared with those in the negative control group. Silencing of circ-0004904 inhibited autophagy, and induced migration and proliferation in JEG3 cells compared with those in the negative control group. In addition, circ-0004904 regulated the levels of ATG12 via interaction with miR-570. Furthermore, circ-0004904 regulated the FUS/VEGF axis in HTR8 and JEG3 cells. In conclusion, circ-0004904 was abnormally expressed in the plasma and placental tissues of patients with preeclampsia. In addition, circ-0004904 was involved in the regulation of proliferation, invasion and autophagy in HTR8 and JEG3 cells. Thus, circ-0004904 may be used as a potential diagnostic biomarker and therapeutic target for preeclampsia.

Correspondence to: Professor Xinghui Liu, Department of Obstetrics, West China Hospital of Sichuan University, 1416 Section 1, Chenglong Avenue, Chengdu, Sichuan 610041, P.R. China
E-mail: xinghuiliu@163.com

Key words: circular RNA 0004904, microRNA-570, invasion, autophagy, VEGF

Introduction

Preeclampsia is a systemic disease during pregnancy, with a global incidence of ~8% in 2019 (1-3). Severe complications of preeclampsia, such as eclampsia and HELLP syndrome, are the most common causes of maternal and perinatal infant death (4). However, to date, the etiology and underlying pathogenic mechanism of preeclampsia remain elusive. Termination of pregnancy currently the only effective treatment measure, especially for severe early-onset preeclampsia, which may cause maternal complications and iatrogenic preterm birth (5,6). Early diagnosis and specific treatment of preeclampsia are severely restricted owning to its unclear pathogenic mechanism (7).

Circular (circ)RNAs participate in the occurrence and development of a variety of diseases, such as Alzheimer's disease, hypertrophic osteoarthropathy, and atherosclerosis (8). Previous studies have demonstrated that abnormal expression of circRNAs is associated with tumor occurrence, invasion, proliferation and metastasis (9-12). For instance, hsa_circ_100395 regulates the proliferation, migration and invasion of lung cancer cells through the microRNA (miRNA/miR)-1228/transcription factor 21 pathway (13). In addition, circRNA La-ribonucleoprotein 4 is considered to act as a miR-424 sponge to inhibit the biological behavior of gastric cancer (14). Other biological functions of circRNAs include chemotherapy resistance and radiosensitivity (15). Abnormally expressed circRNAs have been reported to exhibit high sensitivity and specificity as diagnostic markers (16-18). For instance, hsa_circRNA_103809 and hsa_circRNA_104700 may be involved in the occurrence of colorectal cancer and can be used as effective biomarkers to diagnose colorectal cancer (19). In addition, circRNAs affect cisplatin resistance in non-small cell lung cancer (20).

Mounting evidence has revealed that abnormal expression of circRNAs serves pivotal roles in preeclampsia. For instance, hsa_circ_0036877 may be used as a potential biomarker for early diagnosis of preeclampsia (21). In addition, hsa_circ_0001438, hsa_circ_0001326 and hsa_circ_32340 serve crucial roles in the progression of preeclampsia (22). Compared

with normal pregnancy, the levels of circRNA-0004904 are increased in the plasma of patients with preeclampsia and may be a potential biomarker for diagnosing preeclampsia (23). However, the role of circRNA-0004904 in preeclampsia has not been fully elucidated. Therefore, the present study aimed to determine the role of circRNA-0004904 in preeclampsia and to clarify its underlying pathogenic mechanism of action.

Materials and methods

Study subjects and placental tissue collection. The present study was approved by the Ethics Committee of the West China Hospital of Sichuan University (Chengdu, China), and all patients signed written informed consent forms prior to the commencement of the study. The placenta tissues were obtained from pregnant women who were admitted to the West China Hospital of Sichuan University between January 2018 and January 2019. The diagnosis of patients with preeclampsia complied with The American College of Obstetricians and Gynecologists Practice Bulletin 2019 (3). The control group comprised women with normal pregnancy, and those with pregnancy diseases were excluded. The ages of pregnant women in the two groups ranged between 24-38 years, with a mean age of 28 years. There was no statistical difference in the age of pregnant women between the two groups. Placental tissues (1 cm^3) and serum samples were collected from 30 pregnant women with preeclampsia and 30 normal parturients with the same gestational age (control group).

Cell culture, transfection and reagents. HTR-8 (cat. no. CRL-3271) and JEG-3 (cat. no. HTB-36) cells were obtained from the American Type Culture Collection and cultured in Dulbecco's modified Eagle's medium (cat. no. D5796; MilliporeSigma), containing 10% fetal bovine serum (cat. no. 16000-044; Gibco; Thermo Fisher Scientific, Inc.) and 1% penicillin/streptomycin (cat. no. C0222; Beyotime Institute of Biotechnology). The cells were incubated at 37˚C in presence of 5% CO_2. The circRNA-0004904-targeting small interfering (si)RNA (siRNA-001 and siRNA-002), negative control siRNA (siNC), and lentivirus-mediated circRNA-0004904 overexpression (OE) vector with its corresponding negative control (OE-NC) were supplied by Shanghai GenePharma Co., Ltd. The sequences of the siRNAs were as follows: siRNA-001, 5'-GCAAATTCCAGA GAGCACGTT-3'; siRNA-002, 5'-AAATTCCAGAGAGCA CGTTTT-3'; and siNC, 5'-UUCUUCGAAGGUGUCACG UTT-3'. Plasmid expression vectors for the overexpression of fused in sarcoma (FUS) and autophagy-related 12 (ATG12) (accession nos. NM_004960 and NM_004707, respectively) were constructed by GeneCopoeia, Inc. In addition, siATG7 (5'-GGUCAAAGGACGAAGAUAACA-3'), siFUS-1 (5'-GGCUAUGGAACUCAGUCAACU-3'), siFUS-2 (5'-GGACAGCAGCAAAGCUAUAAU-3'), hsa-miR-570-3p mimics (cat. no. HmiR-SN0669), mimics control (cat. no. CmiR-SN0001-SN), hsa-miR-570-3p inhibitor (cat. no. HmiR-AN0669-SN-10) and inhibitor control (cat. no. CmiR-AN0001-SN) were obtained from GeneCopoeia, Inc. For transfections, cells were seeded in a 6-well plate ($1x10^5$ cells/well). When the cells were ~80% confluent, 2 μg plasmids were transfected using the EndoFectin™ MAX transfection reagent (cat. no. EFM1004-01; GeneCopoeia, Inc.) for 24 h at 37˚C. The mRNA or protein levels were detected at 48 h post-transfection.

RNA pull-down assay. A circRNA-0004904 probe was used for RNA pull-down assay (cat. no. A04001; GenePharma Co., Ltd.) as previously described (24). Cells were lysed using RIPA Lysis Buffer (cat. no. P0013D, Beyotime Biotechnology). RNA pulldown assay was performed using Pierce™ Magnetic RNA-Protein Pull-Down Kit (cat. no. 20164; Thermo Fisher Scientific, Inc.) according to the manufacturer's instructions with 20 μl lysate per reaction. The miRNA level was detected by reverse transcription-quantitative (RT-q)PCR.

RT-qPCR. RT-qPCR was performed as previously described (24). Total RNA was extracted from cells and tissues using TRIzol® reagent (Takara Biotechnology Co., Ltd.) according to the manufacturer's instructions. For miRNA analysis, cDNA was obtained using the All-in-One™ miRNA First-Strand cDNA Synthesis kit (cat. no. QP013; GeneCopoeia, Inc.), and RT-qPCR was performed using the All-in-One™ miRNA qRT-PCR Detection kit (cat. no. QP015; GeneCopoeia, Inc.). U6 small nuclear RNA was used as an endogenous control for normalization. For circRNA analysis, cDNA was synthesized from 1 μg total RNA using the All-in-One First Strand Synthesis kit (cat. no. AORT-0020; GeneCopoeia, Inc.). The real-time PCR kit was purchased from GeneCopoeia, Inc. qPCR was performed under the following conditions: Initial denaturation at 95˚C for 10 min, followed by 35 cycles of 95˚C for 10 sec and 60˚C for 20 sec, and a final extension at 72˚C for 10 sec. qPCR was conducted using the PCR System (Bio-Rad Laboratories, Inc.) according to the manufacturer's instructions. Each experiment was performed in triplicate. Gene expression analysis was performed using the $2^{-\Delta\Delta Cq}$ method (25). The circ-0004904 primers (5'-CCTCCGGTGATAGGTTCTCA-3' and 3'-TAAATTTGGTGCAGGGTGGT-5') were synthesized by Shanghai GenePharma Co., Ltd. Primers for ATG12 (cat. no. HQP055328), GAPDH (cat. no. HQP064347), miR-570 (cat. no. HmiRQP0669) and U6 (cat. no. HmiRQP9001) were purchased from GeneCopoeia, Inc.

Western blot assay. Protein expression levels of ATG12, GAPDH, LC3-II, P62, FUS and vascular endothelial growth factor (VEGF) were detected by western blotting. The transfected HTR-8 and JEG-3 cells were cultured in 6-well plates and lysed at 48 h post-transfection with radio-immunoprecipitation assay lysis buffer (MilliporeSigma) containing phosphatase and protease inhibitors. Protein quantification was performed using BCA assay. Proteins (20 μg/lane) were separated by 10% SDS-PAGE and transferred to PVDF membranes. The membranes were blocked with 5% BSA for 1 h at room temperature and incubated overnight at 4˚C with the following primary antibodies (dilution, 1:1,000): Rabbit monoclonal anti-ATG12 (cat. no. ab109491; Abcam), rabbit recombinant monoclonal GAPDH (cat. no. ab181602; Abcam), rabbit recombinant monoclonal LC3-II (cat. no. ab192890; Abcam), rabbit recombinant monoclonal anti-P62 (cat. no. ab109012; Abcam), rabbit recombinant monoclonal FUS (cat. no. ab124923; Abcam) and rabbit recombinant monoclonal VEGF (cat. no. AB1876-I; Sigma-Aldrich; Merck KGaA). Following

washing for 3x10 min using the Western Wash Buffer (cat. no. P0023C3; Beyotime Institute of Biotechnology) at room temperature, HRP-conjugated secondary antibodies (1:2,000; cat. no. 7074; Cell Signaling Technology, Inc.) were applied to the membranes for 1 h at room temperature, and chemiluminescent signals of membranes were measured by using an ImageQuant LAS system (GE Healthcare). Densitometric analysis was performed using Image Lab (version 3.0, Bio-Rad Laboratories). All experiments were performed in triplicate and repeated three times.

Matrigel invasion assay. Matrigel invasion assay was performed to assess the invasive ability of HTR8 or JEG3 cells as previously described (26,27). The upper chamber of the 24-well Transwell insert was pre-coated with 100 μl diluted Matrigel at 37˚C for 5 h. A total of 1x10^5 HTR8 or JEG3 cells resuspended in serum-free medium were seeded into the upper chamber. The lower chambers contained medium with 10% fetal bovine serum. The cells were incubated at 37˚C for 24 h. Subsequently, cotton swabs were used to remove the non-invasive cells. The migrated cells attached to the lower surface of the membrane were fixed with 4% paraformaldehyde and stained with 0.5% crystal violet for 15 min at room temperature. The cells that migrated to the lower chamber were observed under an optical microscope (x20 magnification). Finally, the crystal violet on the membrane was solubilized with 500 μl 33% acetic acid solution. The optical density of the plates was measured at 595 nm wavelength using a microplate reader.

Fluorescence in situ hybridization (FISH) assay. The source of template was total RNA of circRNA0004904 (sequence, 5'-AGAGCACGTTTTCAATATCATAGGAGCATTTGATAT TCCACGCTTTGTGTACAATTCAGAAAGAAAAAAATT TCTTCCTCTGTTAATGACCAACCACCCTGCACCAAATTTATT TGGAACACCAAGAGATAAAGCAGAGATGTTTCGTGA GCGATATACCATTTTGCACCAGAGGACCCACAGGCA TGAATTATTTACTCCTCCGGTGATAGGTTCTCACCC TGATGAAAGCGGAAGCAAATTCCAG-3'). A Cy3-labeled probe against circRNA0004904 (sequence, 5'-CUCCUAUGA UAUUGAAAACGUGCUCUCUGGAAUUUGCUUCCGC UUUCAUC-3') and a FITC-labeled probe against miR-570 (sequence, 5'-CAAAGGUAAUUGCUGUUUUCG-3') were synthesized by Shanghai GeneChem Co., Ltd. The FISH assay was conducted according to the manufacturer's instructions provided with a FISH kit (cat. no. F32201; Shanghai GeneChem Co., Ltd.) (28,29). HTR8 cells (2x10^5) were fixed with absolute ethanol to in a 48-well plate at room temperature for 15 min, followed by treatment with 100 μl 0.1% Triton x-100 at room temperature for 15 min. Gradient ethanol dehydration (70, 85 and 100%). Subsequently, denaturation was performed at 73˚C for 5 min. A total of 100 μl probe mixture was added and incubated overnight at 37˚C. The next day, the probe mixture was removed, 100 μl 0.4X saline sodium citrate/0.3% Tween-20 was added, and the cells were washed twice at room temperature for 5 min. Finally, 100 μl Hoechst stain was added to each well for 15 min at room temperature. Confocal images were acquired using a laser-scanning confocal microscope (x400 magnification). A total of five fields were imaged per sample. All experiments were performed in triplicate and repeated three times.

Dual-luciferase reporter assay. Dual-luciferase receptor assay was performed using the Dual-Luciferase Reporter Assay system (Promega Corporation). In brief, 2.5x10^5 HTR8 cells were harvested in a 24-well plate. A total of 2 μg wild-type or mutant circ-000490 reporter was constructed by Shanghai GeneChem Co., Ltd. and co-transfected with 100 nM miR-570 or miR-NC and the *Renilla* plasmid using EndoFectin™ MAX transfection reagent (cat. no. EFM1004-01; GeneCopoeia, Inc.) for 24 h at 37˚C. Luciferase activity was detected at 48 h post-transfection. Firefly luciferase activity was normalized to that of *Renilla* luciferase. All experiments were performed in triplicate and repeated three times.

Tandem fluorescent-tagged LC3 (mRFP-EGFP-LC3). A total of 1x10^5 JEG3 cells were co-transfected with mRFP-GFP-LC3 and siNC, siRNA-001 or siRNA-002 using the EndoFectin™ MAX transfection reagent for 24 h at 37˚C and cultured for 22 h. Subsequently, the cells were treated with Earle's balanced salts solution for 2 h at 37˚C. HTR8 cells were co-transfected with mRFP-GFP-LC3 and OE or OE-NC using the EndoFectin™ MAX transfection reagent for 24 h at 37˚C and analyzed by confocal microscopy after 24 h. LC3 dots were quantified using the image pro-plus 6.0 software. All experiments were performed in triplicate and repeated three times. To evaluate the autophagic flux, 3-MA and chloroquine (CQ) were used. At 48 h post-transfection, 5 mM 3-MA or 50 μM CQ were added to the medium for 12 h at 37˚C, and LC3 protein expression levels were detected by western blotting.

5-Ethynyl-2'-deoxyuridine (EdU) assay. A total of 1x10^5 HTR-8 cells were seeded into a 24-well plate and treated with 200 μl EdU (dilution, 1:1,000) in the dark for 1 h at 37˚C using the BeyoClick™ EdU Cell Proliferation kit (Beyotime Institute of Biotechnology) according to the manufacturer's instructions. The cells were washed with PBS (5 min three times). Hoechst 33342 (Beyotime Institute of Biotechnology) was used for nuclear staining (30). Subsequently, the cells were visualized under a fluorescence microscope (x200 magnification; Olympus Corporation). A total of five fields were analyzed per sample.

Bioinformatics. The interaction between circ-0004904 and miRNAs was predicted using the CircInteractome database (https://circinteractome.nia.nih.gov/) (31). The binding site between ATG12 and miR-570 was predicted by TargetScan (32,33).

Statistical analysis. All statistical analyses were performed using SPSS software version 17.0 (SPSS, Inc.). Data are presented as the mean ± SD or SEM. Statistical analysis was performed by the unpaired Student's t-test or one-way ANOVA with Tukey's post hoc test. $P<0.05$ was considered to indicate a statistically significant difference.

Results

Expression levels of circ-0004904 are increased in placental tissues and plasma samples of patients with preeclampsia. The expression levels of circ-0004904 were detected in the

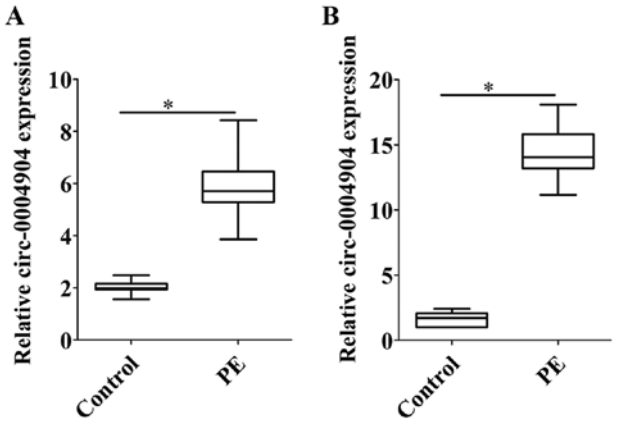

Figure 1. Expression of circ-0004904 is upregulated in placental tissues and plasma samples of patients with PE compared with those in samples from control subjects. (A and B) The expression levels of circ-0004904 were detected in (A) placental tissues and (B) plasma samples of 30 patients with PE and 30 normal parturients with the same gestational age by reverse transcription-quantitative PCR. Data are presented as the mean ± SEM. *P<0.05. PE, preeclampsia; circ, circular RNA.

placental tissues and plasma samples of 30 patients with preeclampsia and 30 normal parturients with the same gestational age. The results demonstrated that the expression levels of circ-0004904 were upregulated in the placental tissues and plasma samples of patients with preeclampsia compared those in the control group (Fig. 1A and B).

circ-0004904 regulates autophagy, proliferation and migration of HTR8 and JEG3 cells. The roles of circ-0004904 were investigated in HTR8 and JEG3 cells. First, the expression levels of circ-0004904 were detected in HTR8 and JEG3 cells. The results revealed that the expression levels of circ-0004904 in JEG3 cells were higher compared with those in HTR8 cells. Silencing or ectopic expression of circ-0004904 significantly inhibited or elevated the expression levels of circ-0004904, respectively (Fig. S1A and B). By contrast, silencing or ectopic expression of circ-0004904 did not affect apoptosis (data not shown). The results also demonstrated that silencing of circ-0004904 repressed LC3-II expression, and promoted the proliferation and migration of JEG3 cells (Figs. 2A, C and S2). By contrast, ectopic expression of circ-0004904 upregulated the levels of LC3-II expression, and inhibited the proliferation and migration of HTR8 cells (Figs. 2B, D and S2). In order to evaluate the effects of circ-0004904 on autophagic flux, 3-MA and CQ were used; the results demonstrated that autophagy mediated by circ-0004904 was inhibited by 3-MA, but not CQ in HTR8 cells (Fig. 2E and F), which suggested that circ-0004904 affected autophagosomes rather than autophagolysosomes. In addition, mRFP-GFP-LC3 was used to detect autophagic flux, and the results revealed that silencing of circ-0004904 inhibited autophagic flux in JEG3 cells (Fig. 2G), whereas overexpression of circ-0004904 promoted autophagic flux in HTR8 cells (Fig. 2H).

circ-0004904-mediated autophagy inhibits the proliferation and invasion of HTR8 cells. Since circ-0004904 promoted autophagic flux in HTR8 cells, the present study further assessed whether circ-0004904-mediated autophagy may regulate cell proliferation and invasion. The results demonstrated that ectopic expression of circ-0004904 inhibited the proliferation and invasion of HTR8 cells. However, following the silencing of ATG7 or the addition of 3-MA, cell proliferation and invasion was partially promoted (Fig. 3A-D). These results suggested that circ-0004904-mediated autophagy inhibited cell proliferation and invasion.

circ-0004904 interacts with miR-570. Bioinformatics analysis predicted that circ-0004904 interacted with a number of miRNAs, including miR-494, miR-513a-3p, miR-570, miR-572, miR-589 and miR-876-3p. The results of the RNA pull-down assays confirmed that circ-0004904 directly bound miR-570 (Fig. 4A). In addition, circ-0004904 was mainly located in the cytoplasm, and circ-0004904 and miR-570 were co-localized in the cytoplasm in HTR8 cells (Fig. 4B). Following silencing of circ-0004904, the expression levels of miR-570 were increased in JEG3 cells compared with those in the cells transfected with siNC (Fig. 4C). By contrast, ectopic expression of circ-0004904 inhibited the expression levels of miR-570 in HTR8 cells compared with those in cells transfected with the OE-NC vector (Fig. 4D). Co-transfection with miR-570 mimics and a wild-type circ-0004904 vector inhibited luciferase activity compared with that observed following transfection with the NC mimics in HTR8 cells (Fig. 4E).

circ-0004904 regulates ATG12 via miR-570. Based on the results of the bioinformatics analysis, ATG12 was selected as a potential target of miR-570. Transfection with miR-570 inhibitors or mimics significantly inhibited or elevated the levels of miR-570 compared with those in the corresponding NC groups (Fig. S1C and D). The results also revealed that transfection with the miR-570 mimics downregulated the mRNA and protein expression levels of ATG12 in HTR8 cells compared with those in the NC group (Fig. 5A), whereas transfection with the miR-570 inhibitors upregulated the expression levels of ATG12 (Fig. 5B). The dual-luciferase reporter assay confirmed that ATG12 was the target of miR-570 in HTR8 cells (Fig. 5C). In addition, circ-0004904 positively regulated the expression levels of ATG12 in HTR8 cells (Fig. 5D and E). However, following transfection with the miR-570 inhibitors, this regulation was partly blocked in HTR8 cells (Fig. 5F and G).

circ-0004904 regulates autophagy via ATG12. The present study further attempted to determine whether circ-0004904 regulated autophagy via ATG12. Silencing or ectopic expression of ATG12 significantly inhibited or elevated, respectively, the mRNA and protein levels of ATG12 compared with those in the corresponding NC groups (Fig. S1E and F). Further results demonstrated that overexpression of circ-0004904 promoted the expression of LC3-II in HTR8 cells compared with that in the NC group, whereas following silencing of ATG12, this regulation was partly suppressed (Fig. 6A). In addition, silencing of circ-0004904 inhibited the expression of LC3-II in JEG3 cells compared with that in the cells transfected with siNC; however, following overexpression of ATG12, the downregulation was reversed (Fig. 6B).

circ-0004904 regulates the FUS/VEGF axis. The present study identified that circ-0004904 directly bound to the FUS protein

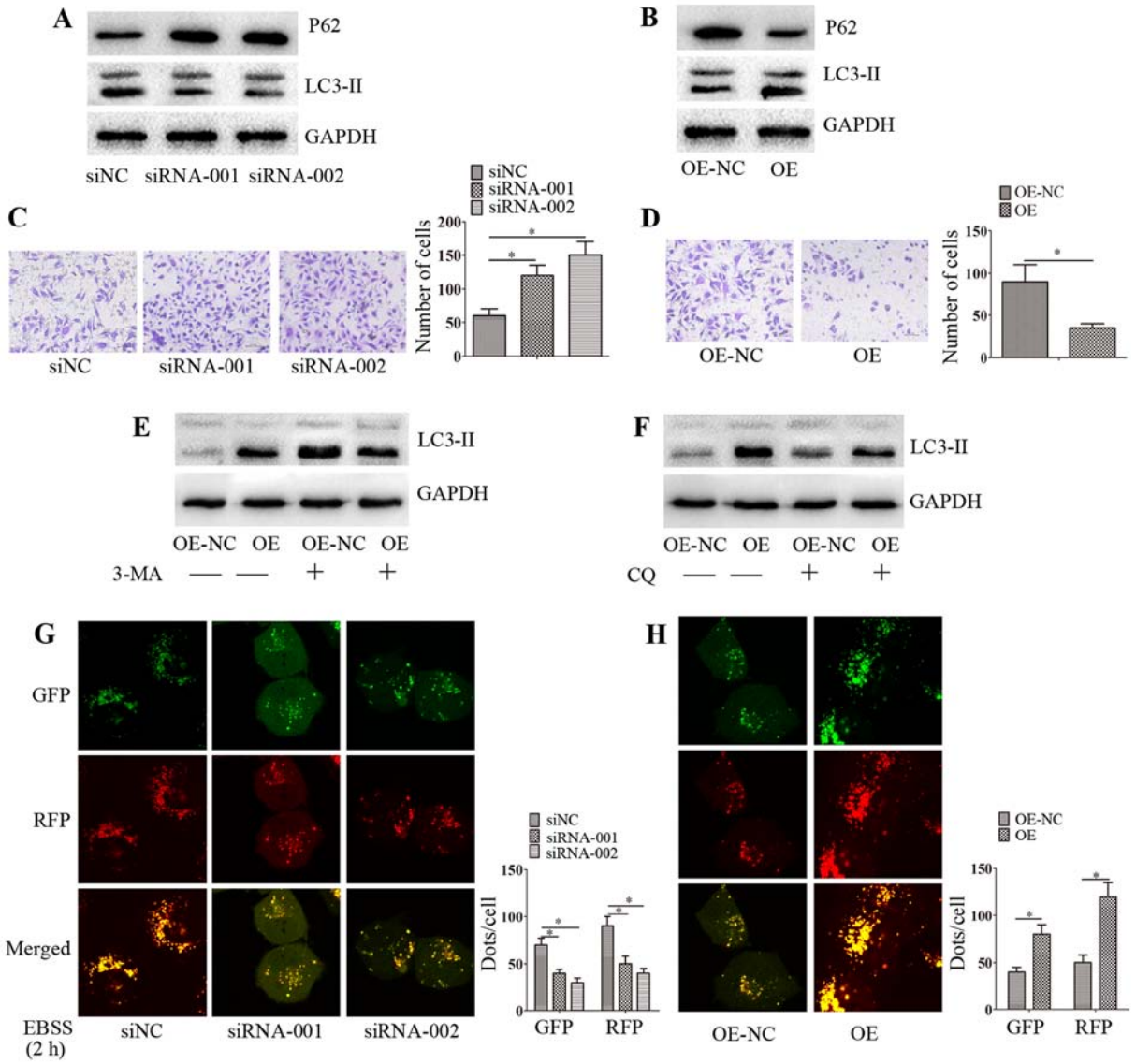

Figure 2. circ-0004904 promotes autophagy and inhibits migration in HTR8 cells. (A and B) The expression levels of LC3-II and P62 were determined by western blotting in (A) JEG3 cells transfected with siNC, siRNA-001 or siRNA-002 and (B) HTR8 cells transfected with OE-NC or OE. (C and D) The invasive ability was assessed by Matrigel invasion assay in (C) JEG3 cells transfected with siNC, siRNA-001 or siRNA-002 and (D) HTR8 cells transfected with OE-NC or OE. (E and F) HTR8 cells were transfected with OE-NC or OE were treated with (E) 3-MA or (F) CQ for 24 h, and the expression levels of LC3-II were detected by western blotting. (G and H) The distribution of mRFP-GFP-LC3 in (G) JEG3 cells transfected with siNC, siRNA-001 or siRNA-002 and (H) HTR8 cells transfected with OE-NC or OE was analyzed by confocal microscopy. Data are presented as the mean ± SEM. *P<0.05. circ, circular RNA; siRNA, small interfering RNA; siNC, negative control siRNA; OE, overexpression vector; OE-NC, negative control vector; GFP, green fluorescent protein; RFP, red fluorescent protein; EBSS, Earle's balanced salt solution.

by bioinformatics analysis. A previous study has reported that FUS inhibits VEGF expression (34); thus, we hypothesized that circ-0004904 may regulate the FUS/VEGF axis. RNA pull-down assay confirmed that circ-0004904 directly bound to the FUS protein (Fig. 7A). Additionally, following silencing of circ-0004904, the expression levels of FUS decreased, whereas the expression levels of VEGF increased in JEG3 cells compared with those in cells transfected with siNC (Fig. 7B). Following ectopic expression of circ-0004904 in HTR8 cells, the expression levels of FUS increased, whereas the levels of VEGF reduced compared with those in the NC group (Fig. 7C). The results also demonstrated that silencing or ectopic expression of FUS significantly inhibited or elevated, respectively, the mRNA and protein levels of FUS compared with those in the corresponding NC groups (Fig. S1G and H). In addition, silencing of FUS increased the expression levels of VEGF compared with those in the siNC group, whereas overexpression of FUS exerted an opposite effect (Fig. 7D and E). When FUS was silenced or overexpressed, this regulation was partially reversed, suggesting that the regulatory effect of circ-0004904 on VEGF protein was dependent on FUS (Fig. 7F and G).

Discussion

Although there are currently reports that circRNA serves a role in the pathogenesis of preeclampsia, the function of circRNA in the occurrence and development of preeclampsia still requires in-depth studies. The results of the present study demonstrated increased expression levels of circ-0004904

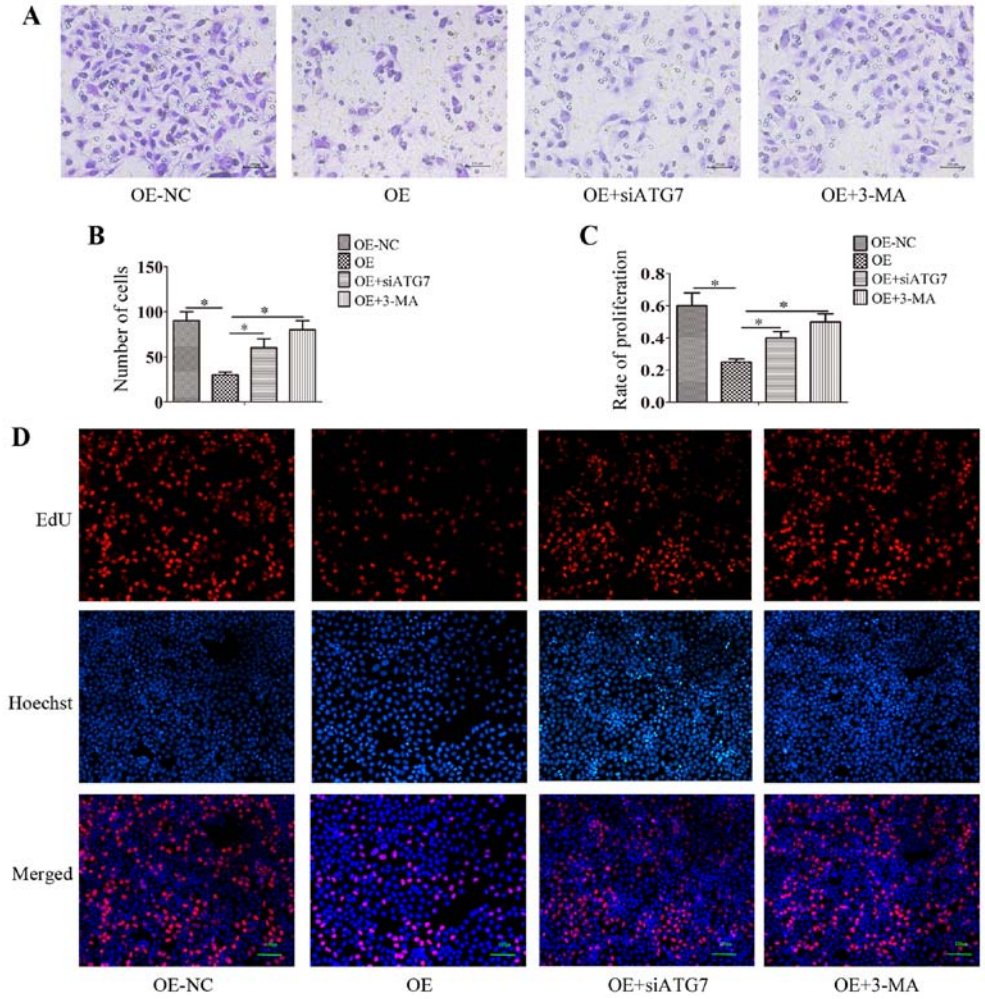

Figure 3. circ-0004904-mediated autophagy inhibits the proliferation and invasion of HTR8 cells. (A and B) HTR8 cells were transfected with OE or OE-NC plasmids, co-transfected with OE + siATG7 or transfected with the OE plasmid and treated with 3-MA, and the cell invasive ability was assessed by Matrigel invasion assay. (A) representative images; (B) mean number of invasive cells. (C and D) HTR8 cells were transfected with OE, OE-NC or OE + siATG7, or transfected with OE and treated with 3-MA, and the cell proliferative ability was determined by EdU assay. (C) Mean number of proliferation cells; (D) representative images. Data are presented as the mean ± SEM. *P<0.05. circ, circular RNA; si, small interfering RNA; OE, overexpression vector; OE-NC, negative control vector; ATG7, autophagy-related 7.

in the placental tissues and plasma samples of patients with preeclampsia compared with those in samples from the control subjects. In addition, circ-0004904 activated autophagy and promoted cellular invasion in the HTR8 and JEG-3 cell lines. It also was revealed that circ-0004904 positively regulated the expression of ATG12 via miR-570. Additionally, circ-0004904 regulated the FUS/VEGF axis (Fig. S3). These results suggested that circ-0004904 may be used as a candidate diagnostic biomarker for preeclampsia and a potential therapeutic target.

Previous studies have demonstrated that autophagy is involved in the occurrence and development of preeclampsia (35-37). The expression levels of LC3, Beclin-1 and total numbers of autophagosomes are upregulated in the placental tissues of patients with preeclampsia compared with those in healthy control subjects, as well as in HTR8 cells and human umbilical vein endothelial cells treated with glucose oxidase compared with those in untreated cells (38,39), suggesting a certain association between autophagy activation and the occurrence of preeclampsia. In the current study, high expression levels of circ-0004904 promoted autophagy, which suggested that highly expressed circ-0004904 may promote the occurrence and progression of preeclampsia. A previous study has confirmed that excessive autophagy inhibits trophoblast invasion and vasculature, thereby causing the onset of preeclampsia (40). In the current study, ectopic expression of circ-0004904 inhibited the invasion of HTR8 cells compared with that in the NC group. Therefore, we hypothesized that the abnormally expressed circ-0004904-mediated autophagy may inhibit the invasion of trophoblasts, thereby participating in the occurrence and development of preeclampsia.

ATG12 is crucial for autophagosome formation, basal autophagy, late endosome-to-lysosome trafficking and exosome release (41,42). In the current study, circ-0004904 promoted autophagic flux, and this regulation was dependent on ATG12. A previous study has reported that miR-570-3p regulates the metastatic effects of metformin on human osteosarcoma by directly targeting ATG12 (43). In the present study, miR-570-3p was demonstrated to mediate the expression of ATG12 by directly targeting ATG12 in HTR8 cells, which was consistent with the findings of a previous study (43). In addition, the results of the present study demonstrated that

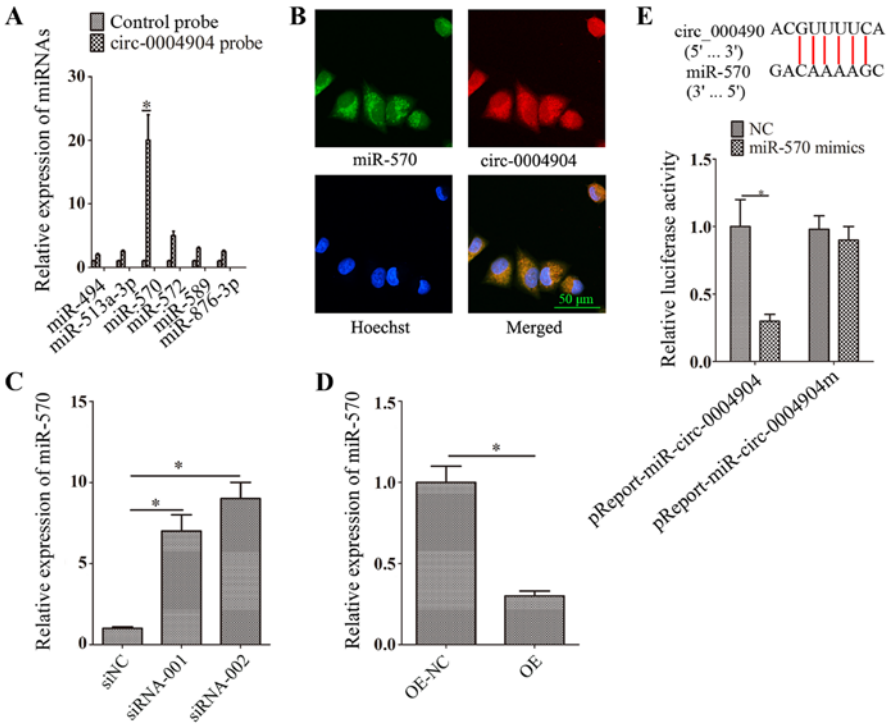

Figure 4. circ-0004904 interacts with miR-570. (A) Bioinformatics analysis predicted that circ-0004904 interacted with miR-494, miR-513a-3p, miR-570, miR-572, miR-589 and miR-876-3p. The interaction between circ-0004904 and miR-570 was assessed using RNA pull-down assay. Expression levels of miRNAs were detected by RT-qPCR. (B) Fluorescence *in situ* hybridization assay was used to identify the colocalization of circ-0004904 and miR-570. Green, FITC-labeled miR-570 probe; red, Cy3-labeled circ-0004904 probe. (C and D) The expression levels of miR-570 were determined by RT-qPCR in (D) JEG3 cells transfected with siNC, siRNA-001 or siRNA-002 and (D) HTR8 cells transfected with OE-NC or OE. (E) Dual-luciferase reporter assay was used to confirm the interaction between circ-0004904 and miR-570. Data are presented as the mean ± SEM. *P<0.05. circ, circular RNA; miR, microRNA; siRNA, small interfering RNA; siNC, negative control siRNA; OE, overexpression vector; NC, negative control; RT-qPCR, reverse transcription-quantitative PCR.

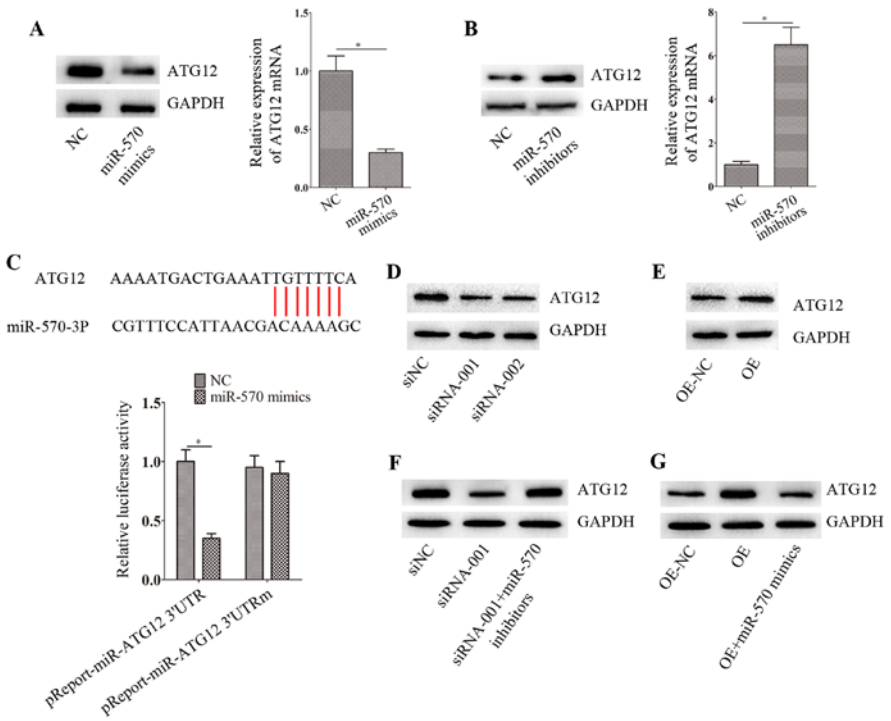

Figure 5. circ-0004904 regulates ATG12 via miR-570. (A and B) The mRNA and protein levels of ATG12 were determined by reverse transcription-quantitative PCR and western blotting, respectively, in HTR8 cells transfected with (A) NC or miR-570 mimics and (B) NC or miR-570 inhibitors. (C) Dual-luciferase reporter assay was used to confirm the interaction between the ATG12 3'-untranslated region and miR-570. (D and E) The expression levels of ATG12 were determined by western blotting in (D) JEG3 cells transfected with siNC, siRNA-001 or siRNA-002 and (E) HTR8 cells transfected with OE-NC or OE. (F and G) The expression levels of ATG12 were determined by western blotting in (F) JEG3 cells transfected with siNC, siRNA-001 or siRNA-001 + miR-570 inhibitors and (G) HTR8 cells transfected with OE-NC, OE or OE + miR-570 mimics. Data are presented as the mean ± SEM. *P<0.05. circ, circular RNA; miR, microRNA; siRNA, small interfering RNA; siNC, negative control siRNA; OE, overexpression vector; NC, negative control; RT-qPCR, reverse transcription-quantitative PCR.

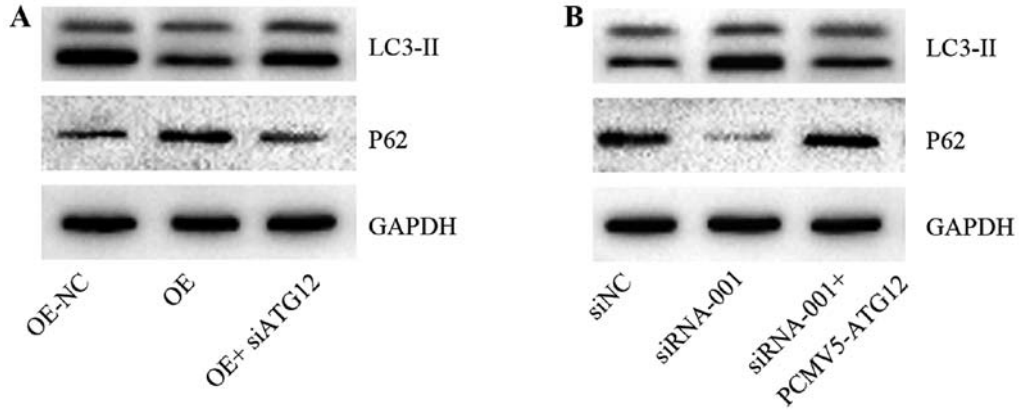

Figure 6. circ-0004904 regulates autophagy via ATG12. (A and B) The expression levels of ATG12 were detected by western blotting in (A) HTR8 cells transfected with OE-NC, OE or OE + siATG12 and (B) JEG3 cells transfected with siNC, siRNA-001 or siRNA-001 + pCMV5-ATG12. circ, circular RNA; siRNA, small interfering RNA; siNC, negative control siRNA; OE, overexpression vector; NC, negative control; ATG12, autophagy-related-12.

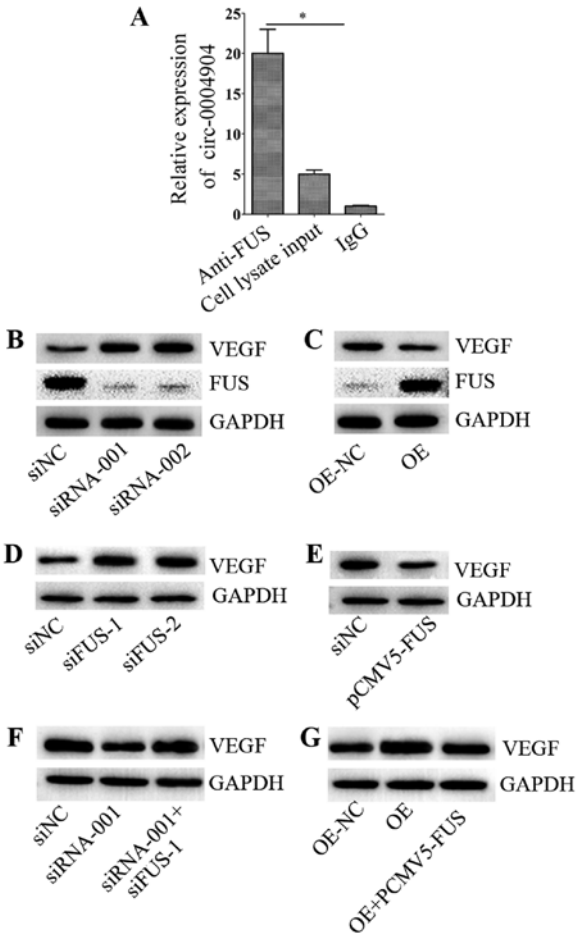

Figure 7. circ-0004904 regulates the FUS/VEGF axis. (A) RNA pull-down assay was used to assess the interaction between circ-0004904 and FUS protein. The expression levels of circ-0004904 were determined by reverse transcription-quantitative PCR. Data are presented as the mean ± SD. (B and C) The expression levels of VEGF and FUS were detected by western blotting in (B) JEG3 cells transfected with siNC, siRNA-001 or siRNA-002 and (C) HTR8 cells transfected with OE-NC or OE. (D and E) The expression levels of VEGF were detected by western blotting in HTR8 cells transfected with (D) NC, siFUS-1 or siFUS-2 and (E) NC or pCMV5-FUS. (F and G) The expression levels of VEGF were detected by western blotting in (F) JEG3 cells transfected with siRNA-001, siNC or siRNA-001 + siFUS-1 and (G) HTR8 cells transfected with OE-NC, OE or OE + pCMV5-FUS. Data are presented as the mean ± SEM. *P<0.05. circ, circular RNA; miR, microRNA; siRNA/si, small interfering RNA; siNC, negative control siRNA; OE, overexpression vector; NC, negative control; FUS, fused in sarcoma.

circ-0004904 regulated ATG12 by sponging miR-570-3p. These results further validated the potential roles of circ-0004904 in promoting autophagy.

A recent study has reported that circRNA fibronectin type III domain-containing 3B directly interacts with FUS and regulates its expression levels (34). In the current study, circ-0004904 directly bound to FUS protein and promoted its expression. Another study has demonstrated that FUS significantly represses tumor growth via inhibiting angiogenesis by reducing the expression levels of VEGF (44). The present results demonstrated that circ-0004904 suppressed the expression level of VEGF, which was dependent on FUS. VEGF is a potential therapeutic target for angiogenesis (45). In placental tissues of patients with preeclampsia, the expression levels of VEGF are downregulated compared with those in healthy subjects (46). Therefore, we hypothesized that high expression levels of circ-0004904 may promote the occurrence and development of preeclampsia.

In conclusion, the results of the present study demonstrated that circ-0004904 was upregulated in the serum samples and placental tissues of patients with preeclampsia compared with those in samples from healthy subjects. High expression levels of circ-0004904 promoted autophagic flux and inhibited cellular invasion *in vitro*. In addition, circ-0004904 regulated the expression levels of ATG12 and VEGF. Therefore, circ-0004904 may be used as a molecular marker for the diagnosis of preeclampsia and a potential therapeutic target. In our future studies, animal models of preeclampsia we will be established to assess the roles and mechanisms of circ-0004904 *in vivo*.

Acknowledgements

Not applicable.

Funding

No funding was received.

Availability of data and materials

All data generated or analyzed during this study are included in the published article.

Authors' contributions

WD designed the study, acquired, analyzed and interpreted the data, drafted and revised the manuscript. XL designed the study, acquired, analyzed and interpreted the data. WD and XL confirm the authenticity of all the raw data. All authors read and approved the final manuscript.

Ethics approval and consent to participate

The present study was approved by the Ethics Committee of the West China Hospital of Sichuan University (Chengdu, China), and all patients signed written informed consent forms prior to the commencement of the study.

Patient consent for publication

Not applicable.

Competing interests

The authors declare that they have no competing interests.

References

1. Chilumula K, Saha PK, Muthyala T, Saha SC, Sundaram V and Suri V: Prognostic role of uterine artery Doppler in early- and late-onset preeclampsia with severe features. J Ultrasound: Aug 24, 2020 (Epub ahead of print). doi: 10.1007/s40477-020-00524-0.
2. Dyess NF and Kinsella JP: Cardiovascular implications for offspring born to mothers with preeclampsia. J Pediatr 228: 11-12, 2021.
3. ACOG Practice Bulletin No. 202: Gestational hypertension and preeclampsia. Obstet Gynecol 133: 1, 2019.
4. Bakrania BA, George EM and Granger JP: Animal models of preeclampsia: Investigating pathophysiology and therapeutic targets. Am J Obstet Gynecol: Nov 23, 2020 (Epub ahead of print). doi: 10.1016/j.ajog.2020.10.025.
5. Jia Y, Xie H, Zhang J and Ying H: Induction of TGF-β receptor I expression in a DNA methylation-independent manner mediated by DNMT3A downregulation is involved in early-onset severe preeclampsia. FASEB J 34: 13224-13238, 2020.
6. Reddy M, Fenn S, Rolnik DL, Mol BW, da Silva Costa F, Wallace EM and Palmer KR: The impact of the definition of preeclampsia on disease diagnosis and outcomes: A retrospective cohort study. Am J Obstet Gynecol 224: 217.e1-217.e11, 2021.
7. Saghafi N, Pourali L, Ghavami Ghanbarabadi V, Mirzamarjani F and Mirteimouri M: Serum heat shock protein 70 in preeclampsia and normal pregnancy: A systematic review and meta-analysis. Int J Reprod Biomed 16: 1-8, 2018.
8. D'Ambra E, Capauto D and Morlando M: Exploring the regulatory role of circular RNAs in neurodegenerative disorders. Int J Mol Sci 20: 5477, 2019.
9. Bai S, Wu Y, Yan Y, Shao S, Zhang J, Liu J, Hui B, Liu R, Ma H, Zhang X and Ren J: Construct a circRNA/miRNA/mRNA regulatory network to explore potential pathogenesis and therapy options of clear cell renal cell carcinoma. Sci Rep 10: 13659, 2020.
10. Dai J, Zhuang Y, Tang M, Qian Q and Chen JP: CircRNA UBAP2 facilitates the progression of colorectal cancer by regulating miR-199a/VEGFA pathway. Eur Rev Med Pharmacol Sci 24: 7963-7971, 2020.
11. Deepthi K and Jereesh AS: An ensemble approach for CircRNA-Disease association prediction based on Autoencoder and deep neural network. Gene 762: 145040, 2020.
12. Gong G, Han Z, Wang W, Xu Q and Zhang J: Silencing hsa_circRNA_0008035 exerted repressive function on osteosarcoma cell growth and migration by upregulating microRNA-375. Cell Cycle 19: 2139-2147, 2020.
13. Chen D, Ma W, Ke Z and Xie F: CircRNA hsa_circ_100395 regulates miR-1228/TCF21 pathway to inhibit lung cancer progression. Cell Cycle 17: 2080-2090, 2018.
14. Zhang J, Liu H, Hou L, Wang G, Zhang R, Huang Y, Chen X and Zhu J: Circular RNA_LARP4 inhibits cell proliferation and invasion of gastric cancer by sponging miR-424-5p and regulating LATS1 expression. Mol Cancer 16: 151, 2017.
15. Wang Y, Zhang J, Li J, Gui R, Nie X and Huang R: CircRNA_014511 affects the radiosensitivity of bone marrow mesenchymal stem cells by binding to miR-29b-2-5p. Bosn J Basic Med Sci 19: 155-163, 2019.
16. Ding C, Yi X, Wu X, Bu X, Wang D, Wu Z, Zhang G, Gu J and Kang D: Exosome-mediated transfer of circRNA CircNFIX enhances temozolomide resistance in glioma. Cancer Lett 479: 1-12, 2020.
17. Wang X, Zhang H, Yang H, Bai M, Ning T, Deng T, Liu R, Fan Q, Zhu K, Li J, *et al*: Exosome-delivered circRNA promotes glycolysis to induce chemoresistance through the miR-122-PKM2 axis in colorectal cancer. Mol Oncol 14: 539-555, 2020.
18. Xiao G, Huang W, Zhan Y, Li J and Tong W: CircRNA_103762 promotes multidrug resistance in NSCLC by targeting DNA damage inducible transcript 3 (CHOP). J Clin Lab Anal 34: e23252, 2020.
19. Bian L, Zhi X, Ma L, Zhang J, Chen P, Sun S, Li J, Sun Y and Qin J: Hsa_circRNA_103809 regulated the cell proliferation and migration in colorectal cancer via miR-532-3p/FOXO4 axis. Biochem Biophys Res Commun 505: 346-352, 2018.
20. Zhao Y, Zheng R, Chen J and Ning D: CircRNA CDR1as/miR-641/HOXA9 pathway regulated stemness contributes to cisplatin resistance in non-small cell lung cancer (NSCLC). Cancer Cell Int 20: 289, 2020.
21. Hu X, Ao J, Li X, Zhang H, Wu J and Cheng W: Competing endogenous RNA expression profiling in pre-eclampsia identifies hsa_circ_0036877 as a potential novel blood biomarker for early pre-eclampsia. Clin Epigenetics 10: 48, 2018.
22. Ou Y, Liu M, Zhu L, Deng K, Chen M, Chen H and Zhang J: The expression profile of circRNA and its potential regulatory targets in the placentas of severe pre-eclampsia. Taiwan J Obstet Gynecol 58: 769-777, 2019.
23. Jiang M, Lash GE, Zhao X, Long Y, Guo C and Yang H: CircRNA-0004904, CircRNA-0001855, and PAPP-A: Potential novel biomarkers for the prediction of preeclampsia. Cell Physiol Biochem 46: 2576-2586, 2018.
24. Han D, Li J, Wang H, Su X, Hou J, Gu Y, Qian C, Lin Y, Liu X, Huang M, *et al*: Circular RNA circMTO1 acts as the sponge of microRNA-9 to suppress hepatocellular carcinoma progression. Hepatology 66: 1151-1164, 2017.
25. Livak KJ and Schmittgen TD: Analysis of relative gene expression data using real-time quantitative PCR and the 2(-Delta Delta C(T)) method. Methods 25: 402-408, 2001.
26. Wang Z, Yu Z, Wang GH, Zhou YM, Deng JP, Feng Y, Chen JQ and Tian L: AURKB promotes the metastasis of gastric cancer, possibly by inducing EMT. Cancer Manag Res 12: 6947-6958, 2020.
27. Xu Y, Ye S, Zhang N, Zheng S, Liu H, Zhou K, Wang L, Cao Y, Sun P and Wang T: The FTO/miR-181b-3p/ARL5B signaling pathway regulates cell migration and invasion in breast cancer. Cancer Commun (Lond) 40: 484-500, 2020.
28. Shang A, Gu C, Wang W, Wang X, Sun J, Zeng B, Chen C, Chang W, Ping Y, Ji P, *et al*: Exosomal circPACRGL promotes progression of colorectal cancer via the miR-142-3p/miR-506-3p-TGF-β1 axis. Mol Cancer 19: 117, 2020.
29. Zhang HD, Jiang LH, Hou JC, Zhong SL, Zhou SY, Zhu LP, Li J, Wang DD, Sun DW, Ji ZL and Tang JH: Circular RNA hsa_circ_0052112 promotes cell migration and invasion by acting as sponge for miR-125a-5p in breast cancer. Biomed Pharmacother 107: 1342-1353, 2018.
30. Xin Y, Min P, Xu H, Zhang Z, Zhang Y and Zhang Y: CD26 upregulates proliferation and invasion in keloid fibroblasts through an IGF-1-induced PI3K/AKT/mTOR pathway. Burns Trauma 8: tkaa025, 2020.
31. Panda AC, Dudekula DB, Abdelmohsen K and Gorospe M: Analysis of circular RNAs using the web tool circinteractome. Methods Mol Biol 1724: 43-56, 2018.
32. Xia L, Li F, Qiu J, Feng Z, Xu Z, Chen Z and Sun J: Oncogenic miR-20b-5p contributes to malignant behaviors of breast cancer stem cells by bidirectionally regulating CCND1 and E2F1. BMC Cancer 20: 949, 2020.
33. Wu YP, Lin XD, Chen SH, Ke ZB, Lin F, Chen DN, Xue XY, Wei Y, Zheng QS, Wen YA and Xu N: Identification of prostate cancer-related circular RNA through bioinformatics analysis. Front Genet 11: 892, 2020.

34. Garikipati VNS, Verma SK, Cheng Z, Liang D, Truongcao MM, Cimini M, Yue Y, Huang G, Wang C, Benedict C, *et al*: Circular RNA CircFndc3b modulates cardiac repair after myocardial infarction via FUS/VEGF-A axis. Nat Commun 10: 4317, 2019.
35. Cornelius DC and Wallace K: Autophagy in preeclampsia: A new target? EBioMedicine 57: 102864, 2020.
36. Nakashima A, Cheng SB, Ikawa M, Yoshimori T, Huber WJ, Menon R, Huang Z, Fierce J, Padbury JF, Sadovsky Y, *et al*: Evidence for lysosomal biogenesis proteome defect and impaired autophagy in preeclampsia. Autophagy 16: 1771-1785, 2020.
37. Zhao H, Gong L, Wu S, Jing T, Xiao X, Cui Y, Xu H, Lu H, Tang Y, Zhang J, *et al*: The inhibition of protein kinase C β contributes to the pathogenesis of preeclampsia by activating autophagy. EBioMedicine 56: 102813, 2020.
38. Akcora Yildiz D, Irtegun Kandemir S, Agacayak E and Deveci E: Evaluation of protein levels of autophagy markers (Beclin 1 and SQSTM1/p62) and phosphorylation of cyclin E in the placenta of women with preeclampsia. Cell Mol Biol (Noisy-le-grand) 63: 51-55, 2017.
39. Oh SY, Choi SJ, Kim KH, Cho EY, Kim JH and Roh CR: Autophagy-related proteins, LC3 and Beclin-1, in placentas from pregnancies complicated by preeclampsia. Reprod Sci 15: 912-920, 2008.
40. Gao L, Qi HB, Kamana KC, Zhang XM, Zhang H and Baker PN: Excessive autophagy induces the failure of trophoblast invasion and vasculature: Possible relevance to the pathogenesis of preeclampsia. J Hypertens 33: 106-117, 2015.
41. Chen ZH, Cao JF, Zhou JS, Liu H, Che LQ, Mizumura K, Li W, Choi AM and Shen HH: Interaction of caveolin-1 with ATG12-ATG5 system suppresses autophagy in lung epithelial cells. Am J Physiol Lung Cell Mol Physiol 306: L1016-L1025, 2014.
42. Murrow L and Debnath J: Atg12-Atg3 coordinates basal autophagy, endolysosomal trafficking, and exosome release. Mol Cell Oncol 5: e1039191, 2018.
43. Bao X, Zhao L, Guan H and Li F: Inhibition of LCMR1 and ATG12 by demethylation-activated miR-570-3p is involved in the anti-metastasis effects of metformin on human osteosarcoma. Cell Death Dis 9: 611, 2018.
44. Deng WG, Kawashima H, Wu G, Jayachandran G, Xu K, Minna JD, Roth JA and Ji L: Synergistic tumor suppression by coexpression of FUS1 and p53 is associated with down-regulation of murine double minute-2 and activation of the apoptotic protease-activating factor 1-dependent apoptotic pathway in human non-small cell lung cancer cells. Cancer Res 67: 709-717, 2007.
45. Lin L, Wang Q, Xu F, Luo X, Xu J, Yan L, Li Q and Hao H: BML-111, the lipoxin A_4 agonist, modulates VEGF or $CoCl_2$-induced migration, angiogenesis and permeability in tumor-derived endothelial cells. Immunol Lett 230: 27-35, 2021.
46. Sahay AS, Jadhav AT, Sundrani DP, Wagh GN, Mehendale SS, Chavan-Gautam P and Joshi SR: VEGF and VEGFR1 levels in different regions of the normal and preeclampsia placentae. Mol Cell Biochem 438: 141-152, 2018.